

Bloch Oscillation under a Bichromatic Laser: Quasi-Miniband Formation, Collapse, and Dynamical Delocalization and Localization

Ren-Bao Liu and Bang-Fen Zhu

*National Laboratory for Superlattices and Microstructures, Institute of Semiconductors,
Chinese Academy of Sciences, P. O. Box 912, Beijing 100 083, People's Republic of China*

A novel DC and AC driving configuration is proposed for semiconductor superlattices, in which the THz AC driving is provided by an intense bichromatic cw laser. The two components of the laser, usually in the visible light range, are near but not exactly resonant with interband Wannier-Stark transitions, and their frequency difference equals the Wannier-Stark ladder spacing. Multi-photon processes with the intermediate states in the conduction (valence) band cause dynamical delocalization and localization of valence (conduction) electrons, and the corresponding formation and collapse of the quasi-minibands.

PACS numbers: 73.20.Dx, 42.50.Hz, 72.20.Ht

Semiconductor superlattices (SSL's) [1] provide a stage for low-dimensional physics and for a variety of ultrafast optoelectronic devices. A typical example for such systems is the well-known Bloch oscillation (BO) [2] and its frequency counterpart, the Wannier-Stark ladder (WSL) [3]. Mainly owing to their long artificial periods, SSL's have been the first systems in which the WSL and BO were observed [5], verifying the early predictions [2,3] based on the band theory [4]. Since the BO is accompanied by a time-dependent dipole momentum, biased SSL's are expected to generate tunable coherent electromagnetic radiation in the THz range [6], which may find extensive applications, e.g., in medical diagnoses. However, the THz emission from Bloch oscillators has turned out to be quite weak, and a strong pulsed laser is required for exciting the wave packets [6], which limits its potential applications.

A THz field has been used to drive the BO, as a result the inverse Bloch oscillators can emit harmonics of the driving field [7,8]. As already reported, the biased SSL's subject to AC-fields exhibit a wealth of interesting physical effects [9–14]. The Hamiltonian of such systems is time-periodic, thus the eigenstates are the Floquet states associated with Floquet indices, i.e. quasienergies, forming the minibands [9–11]. With variation of the THz field strength, the quasi-miniband width oscillates, and will collapse at certain field strengths [9–11]. Correspondingly, the Bloch electrons are dynamically delocalized and localized [9,10,12–14]. Experiments about these effects, however, have been quite scarce [7,8], because it is not easy to obtain an intense THz source such as the free electron laser, which has moreover to be effectively coupled to the SSL's. This also prevents utilization

of the THz driven SSL's in practical devices.

In this Letter, we propose an alternative driving configuration. As schematically illustrated in Fig. 1, a biased SSL is driven by an intense *bichromatic cw* laser with its two components at the frequencies ω_1 and ω_2 , and whose average $\Omega \equiv (\omega_1 + \omega_2)/2$ is nearly resonant with E_g , the frequency of the ground-state excitonic Wannier-Stark transition in the same quantum well, and thus is usually in the *visible light* range. The frequency difference between the two components $2\omega \equiv |\omega_1 - \omega_2|$ is adjusted to ω_{BO} , the BO frequency or WSL spacing, which is in the THz range. Suppose the two components have equal weight, then the optical field can be expressed as

$$\mathbf{E}(t) = 2\mathbf{E}_0 \cos(\omega t) \cos(\Omega t). \quad (1)$$

Here we have assumed the sample to be optically thin and neglected the spatial dependence of the laser. As will be shown later, this SSL can be equivalently described by a time-periodic Hamiltonian with the period $2\pi/\omega$, and in which the dynamical effects are similar to those in the usual DC-biased and AC driven SSL's [9–14].

At this point, it should be pointed out that although, atoms excited by two optical fields have been extensively studied both theoretically and experimentally [15], and the AC Stark effect in semiconductors driven by an intense monochromatic laser is also well understood [16], to the best of our knowledge, there has been no report on Bloch oscillations driven by a bichromatic laser.

In order to keep the following treatment as simple as possible, we have made several simplifications. First, we consider only the ground-state exciton for each Wannier-Stark transition. This is justified because the laser frequencies can be chosen well below the continuum transitions in the same quantum well and also by the fact that the ground-state exciton possesses by far the strongest component of oscillator strength. Secondly, we neglect the unequal WSL spacing effect [5,17] and Fano interference between the continua and the embedded discrete states [18] induced by the Coulomb interaction. Usually, the excitonic coupling affects significantly the dynamical delocalization or localization [13,14], this however will be taken into account in our later work. Thirdly, the Zener tunneling and band mixing effects are not included. And lastly, the laser is assumed detuned for transitions other than those between the highest valence and the lowest conduction minibands. All these assumptions will in some way affect our results. Even so, the principle as well as main conclusions will not be qualitatively modified.

With these simplifications, the Hamiltonian can be mapped into a one-dimensional model with two-band as well as nearest-neighbor coupling. With a well-justified rotating wave approximation for the optical coupling and the unitary transformation

$$S = \exp[i\Omega t \sum_n (a_{cn}^\dagger a_{cn} - a_{vn}^\dagger a_{vn})/2],$$

the Hamiltonian in the rotating frame is

$$H = \sum_n (n\omega_{BO} + \frac{\varepsilon_0}{2}) a_{cn}^\dagger a_{cn} - \frac{\Delta_c}{4} a_{cn}^\dagger (a_{cn+1} + a_{cn-1}) \\ + (n\omega_{BO} - \frac{\varepsilon_0}{2}) a_{vn}^\dagger a_{vn} + \frac{\Delta_v}{4} a_{vn}^\dagger (a_{vn+1} + a_{vn-1}) \\ - \chi \cos(\omega t) (a_{cn}^\dagger a_{vn} + \text{H.c.}), \quad (2)$$

where a_{cn}^\dagger (a_{vn}^\dagger) stands for the operator creating a conduction (valence) electron at the n th site, Δ_c (Δ_v) is the conduction (valence) miniband width, $\varepsilon_0 \equiv E_g - \Omega$ is the detuning, and $\chi \equiv dE_0$ is the interband optical transition strength (d is the interband dipole matrix element along the \mathbf{E}_0 direction). Compared to the usual THz driving WSL system, the driving force in the present configuration is essentially an interband rather than an intraband process.

The time-periodic system described by Eq. (2) has no stationary solution, and the eigenstates are time-periodic Floquet states $|q, m\rangle \equiv \exp(im\omega t)|q\rangle$ with period $T = 2\pi/\omega$, which satisfy

$$(H - i\partial_t)|q, m\rangle = \varepsilon_{q,m}|q, m\rangle,$$

where $\varepsilon_{q,m} \equiv \varepsilon_q + m\omega$ is the Floquet index, i.e. quasienergy. The Floquet states and indices can be obtained by diagonalizing the secular equation

$$U(T, 0)|q\rangle = \exp(-i\varepsilon_q T)|q\rangle,$$

where the propagator

$$U(T, 0) \equiv \hat{T} \exp[-i \int_0^T H(t) dt].$$

The Hamiltonian (2) can be decomposed into a sum of mutually commutative 2×2 matrices in the accelerating quasimomentum representation $\{|\alpha, \tilde{k}\rangle | \alpha = c, v\}$ with the transformation $|\alpha, \tilde{k}\rangle = |\alpha, k - \omega_{BO}t\rangle$ (hereafter the superlattice period is assumed to be unity). That is $H = \sum_k H_k$, with

$$H_k = \sum_{\alpha=c,v} \varepsilon_{\alpha\tilde{k}} a_{\alpha\tilde{k}}^\dagger a_{\alpha\tilde{k}} - \chi \cos(\omega t) (a_{c\tilde{k}}^\dagger a_{v\tilde{k}} + \text{H.c.}), \quad (3)$$

where $\varepsilon_{c\tilde{k}} = (\varepsilon_0 - \Delta_c \cos \tilde{k})/2$ and $\varepsilon_{v\tilde{k}} = (-\varepsilon_0 + \Delta_v \cos \tilde{k})/2$ are the conduction and valence miniband dispersions, respectively. Thus each quasimomentum k corresponds to two sets of Floquet states $|\pm, m\rangle_k$ with the quasienergies $\varepsilon_{k\pm, m}$.

Before we present our numerical results, the quasi-minibands are analytically evaluated in the weak and strong optical coupling limits, so as to give some physical insight. From now on, we will set $E_g = \Omega$.

When $\chi = 0$, i.e. there is no optical field, H_k is already diagonalized, and the quasienergies produce the well-known WSL [3].

When χ is small, the optical coupling

$$H_{1,k} \equiv -\chi \cos(\omega t) (a_{c\tilde{k}}^\dagger a_{v\tilde{k}} + \text{H.c.})$$

can be treated as a perturbation to

$$H_{0,k} \equiv \varepsilon_{c\tilde{k}} a_{c\tilde{k}}^\dagger a_{c\tilde{k}} + \varepsilon_{v\tilde{k}} a_{v\tilde{k}}^\dagger a_{v\tilde{k}}.$$

Similar to the steady case, a perturbation theory can be developed, in which the matrix element for time-periodic functions is defined as

$$\langle\langle q, m | H | q', m' \rangle\rangle \equiv \frac{1}{T} \int_0^T \langle q, m | H | q', m' \rangle dt$$

in the Hilbert subspace [10]. In terms of unperturbed Floquet states

$$|\pm\rangle_k = \exp[\pm i\Delta_{c/v}/(2\omega_{BO}) \sin(\omega_{BO}t - k)] |c/v, \tilde{k}\rangle$$

with the quasienergies $\varepsilon_{k\pm}^{(0)} = 0$, the optical coupling is expressed as

$$k \langle\langle +, m | H_{1,k} | +, m' \rangle\rangle_k = k \langle\langle -, m | H_{1,k} | -, m' \rangle\rangle_k = 0, \quad (4) \\ k \langle\langle -, m | H_{1,k} | +, m' \rangle\rangle_k = k \langle\langle +, m' | H_{1,k} | -, m \rangle\rangle_k^* \\ = -\frac{\chi}{2} \sum_{n,\pm} \delta_{n, \frac{m-m'\pm 1}{2}} J_n\left(\frac{\Delta}{2\omega_{BO}}\right) e^{-ink}, \quad (5)$$

where $\Delta \equiv \Delta_c + \Delta_v$ is the combined miniband width, n is an integer number, and $J_n(x)$ is the n th order Bessel function of the first kind. According to Eq. (4) and (5), the quasienergy spectrum depends on only Δ rather than the ratio Δ_c/Δ_v .

From the symmetry of the matrix elements, the quasienergies $\varepsilon_{k\pm}$ satisfy the relation $\varepsilon_{k\pm} = -\varepsilon_{k\mp} = \varepsilon_{\pi-k\mp} = \varepsilon_{k-\pi\mp} = \varepsilon_{-k\pm}$, so each Floquet state is 4-fold degenerate, and only the quasienergies for $k \in [0, \pi/2]$ need to be calculated to obtain the full spectrum information.

Since the first-order modification for the quasienergies vanishes (Eq. (4)), the second-order perturbation gives

$$\varepsilon_{k\pm} = \mp \chi^2 \cos k \sum_{n=1}^{+\infty} \frac{J_n(\frac{\Delta}{2\omega_{BO}}) J_{n-1}(\frac{\Delta}{2\omega_{BO}})}{(2n-1)\omega}, \quad (6)$$

which forms a miniband. It can be recognized at once that, except for a prefactor, the quasi-miniband has a dispersion relation identical to that of the original minibands. The discrete WSL is broadened, indicating dynamical delocalization of the originally localized Wannier-Stark states.

An intuitive picture favors our understanding of the dynamical delocalization. As depicted in Fig. 1 (b), a valence band electron in a Wannier-Stark state can hop to its neighbor states by first absorbing a photon from one component of the bichromatic laser and then emitting a photon to the other component, though both components are off-resonant with the interband transitions. The square law dependence of the quasi-miniband width on the optical coupling strength χ results from this second-order process, in which a conduction band electron plays the role of an intermediate state. Clearly, the Bessel functions $J_n(\frac{\Delta}{2\omega_{BO}})$ and $J_{n-1}(\frac{\Delta}{2\omega_{BO}})$ in Eq. (6) reflect the two virtual transitions between the intermediate state and the initial and final Wannier-Stark states. A conduction electron can similarly be delocalized.

With increasing laser intensity, multi-photon processes become more and more important, and the perturbation treatment for the optical coupling will fail eventually. Thus, when $\chi \gg \Delta$, the $H_{0,k}$ should be regarded as the perturbation to $H_{1,k}$ [10]. Since eigenstates of $H_{1,k}$ are

$$|\pm\rangle_k = \exp[\pm i\chi/\omega \sin(\omega t)]\sqrt{2}/2(|c, \tilde{k}\rangle \pm |v, \tilde{k}\rangle),$$

the first-order degenerate perturbation gives the quasi-miniband dispersion as

$$\varepsilon_{k\pm} = \pm \frac{\Delta}{4} J_2\left(\frac{2\chi}{\omega}\right) \cos k. \quad (7)$$

In this strong coupling limit, the quasi-miniband width oscillates according to a second order Bessel function with the argument of 2χ over ω , and the quasi-miniband collapses at such laser intensities that $2\chi/\omega$ is a root of the Bessel function, which is very similar to the case of intra-miniband driving by a THz field. The Taylor expansion of the Bessel function in Eq. (7) contains only even powers of χ , indicating that each virtual photon absorption is necessarily followed by a virtual photon emission, and no process with an odd number of photons is involved. This again confirms our intuitive picture invoked to understand the dynamical delocalization.

The formation and collapse of the quasi-miniband can be clearly seen from Fig. 2, in which the quasienergies are numerically calculated as functions of the optical coupling strength for 21 k points taken evenly from 0 to $\pi/2$. For comparison, the perturbation results for $k = 0$ are also plotted. In the weak optical coupling limit ($2\chi/\omega < 2$), the second order perturbation of $H_{1,k}$ (dashed lines) gives results well consistent with the numerical ones. In the strong coupling limit, the first order perturbation of $H_{0,k}$ is also a quite good approximation, especially for smaller Δ , where the requirement for the perturbation treatment $\chi \gg \Delta$ is better met.

Comparing the numerical results with the perturbation calculations, two points need mentioning. First, the quasi-miniband collapses at $2\chi/\omega \approx 4.16, 7.84$, etc. for $\Delta = 33$ meV, and at $2\chi/\omega \approx 4.96, 8.32$, etc. for $\Delta = 16.5$

meV, which correspond to laser intensities a little weaker than the roots of the Bessel function. We think it comes from the underestimated localization effect of the DC field by treating $H_{0,k}$ as a perturbation. Secondly, the numerically calculated band collapse is not as complete as that in perturbation calculations, because of the interaction between different sidebands of the Floquet states of $H_{1,k}$.

To show the dynamical delocalization and localization of a bichromatic laser driven electron, we have calculated the evolution of an initially localized electron by integrating the Schrödinger equation. The wave packet width W defined to characterize the localization of an electron is

$$W^2 \equiv \sum_n (n - r_0)^2 (\langle a_{cn}^\dagger a_{cn} \rangle + \langle a_{vn}^\dagger a_{vn} \rangle),$$

where

$$r_0 \equiv \sum_n n (\langle a_{cn}^\dagger a_{cn} \rangle + \langle a_{vn}^\dagger a_{vn} \rangle).$$

When $t = 0$, the electron is put at the valence site $n = 0$ [19]. With such an initial condition, the wave packet center r_0 is found to be always zero for any laser intensity.

In Fig. 3, W is shown as a function of time within the first ten periods for three laser intensities. Without the optical field (Fig. 3 (a)), the wave packet width W oscillates sinusoidally with time with a static center-of-mass, which is just the breathing mode of the BO [20] and the well-known Wannier-Stark localization. The two non-zero laser intensities correspond to approximately maximum quasi-miniband width and band collapse, respectively. When the quasi-miniband width is a maximum ($2\chi/\omega = 3.04$, Fig. 3 (b)), W increases linearly with time with a slight oscillation superimposed, which clearly evidences the dynamical delocalization of the initially localized electron. When the quasi-miniband collapses ($2\chi/\omega = 4.96$, Fig. 3 (c)), W oscillates with time significantly and quasi-periodically, whose minima are slightly shifted upward due to imperfect band collapse. It is obvious that the dynamical localization is realized.

Note that the dynamical localization length is larger than the Wannier-Stark localization length by a factor of about Δ/Δ_v , which suggests a similar band-width dependence for both kinds of localization. This behavior is also exhibited for dynamical delocalization, which, as shown in Fig. 3 (b), compares very well to the diffusion of a free Bloch electron provided identical bandwidths (≈ 3.9 meV) are adopted.

The population of the conduction miniband $f_c \equiv \sum_n \langle a_{cn}^\dagger a_{cn} \rangle$ is also plotted for $2\chi/\omega = 3.04$ (the dotted line). f_c oscillates nearly periodically with time due to virtual excitation. When a valence band electron is excited into the conduction states, it can hop to neighbor sites, thus W ascends by a step, which confirms once more our intuitive picture for the dynamical delocalization process.

In summary, we have predicted the quasi-miniband formation and collapse, and correspondingly the dynamical delocalization and localization for an electron in a SSL driven by DC and AC fields in a novel configuration, in which the THz AC driving is provided by an intense bichromatic visible laser with the frequency difference of the two components equal to the WSL spacing. Our findings suggest that the experiments on the dynamical effects can be carried out without expensive THz sources like free electron lasers. Suppose $\omega_{BO} = 2\omega = 10$ meV, an optical coupling of 12.4 meV is enough to realize the dynamical localization, which should be accessible already in many laboratories. It should be noted that the two components of the bichromatic laser can be replaced by two independent lasers with small phase fluctuation. The possible THz emission from so driven Bloch oscillators, requiring neither an intense THz source nor pulse optical excitation, may find broad applications. In addition, this interband driving configuration introduces several interesting physical problems such as the excitonic effect and excitation-induced many body correlation, which are absent in the usual intraminiband THz driving configuration.

The authors are grateful to Professor Kun Huang and A. Rhys for their critical reading of the manuscript. This work was supported by the National Science Foundation of China and the QiuShi Science & Technology Foundation of Hong Kong.

and extensive references therein.

-
- [1] L. Esaki and R. Tsu, IBM J. Res. Devel. **14**, 61 (1970).
 - [2] C. Zener, Proc. R. Soc. London Ser. A **145**, 523 (1932).
 - [3] G. H. Wannier, Phys. Rev. **117**, 432 (1960).
 - [4] F. Bloch, Z. Phys. **52**, 555 (1928).
 - [5] E. E. Mendez, F. Agullo-Rueda, and J. M. Hong, Phys. Rev. Lett. **60**, 2426 (1988); P. Voisin *et al.*, *ibid* **61**, 1639 (1988); J. Feldmann *et al.*, Phys. Rev. B **46**, 7252 (1992); V. G. Lyssenko *et al.*, Phys. Rev. Lett., **79**, 301 (1997).
 - [6] C. Waschke *et al.*, Phys. Rev. Lett. **70**, 3319 (1993); T. Dekorsy, P. Leisching, K. Köhler, and H. Kurz, Phys. Rev. B **50**, 8106 (1994); R. Martini *et al.*, *ibid* **54**, 14 325 (1996).
 - [7] B. J. Keay *et al.*, Phys. Rev. Lett. **75**, 4102 (1995).
 - [8] K. Unterrainer *et al.*, Phys. Rev. Lett. **76**, 2973 (1996).
 - [9] M. Holthaus, Phys. Rev. Lett. **69**, 351 (1992).
 - [10] M. Holthaus, Z. Phys. B **89**, 251 (1992).
 - [11] J. Zak, Phys. Rev. Lett. **71**, 2623 (1993).
 - [12] A. A. Ignatov and Y. A. Romanov, Phys. Status Solidi (B) **73**, 327 (1976); D. H. Dunlap and V. M. Kenkre, Phys. Rev. B **34**, 3625 (1986).
 - [13] T. Meier, F. Rossi, P. Thomas, and S.W. Koch, Phys. Rev. Lett. **75**, 2558 (1995).
 - [14] R.-B. Liu and B.-F. Zhu, Phys. Rev. B **59**, 5759 (1999).
 - [15] A. S. M. Windsor *et al.*, Phys. Rev. Lett. **80**, 3045 (1998),

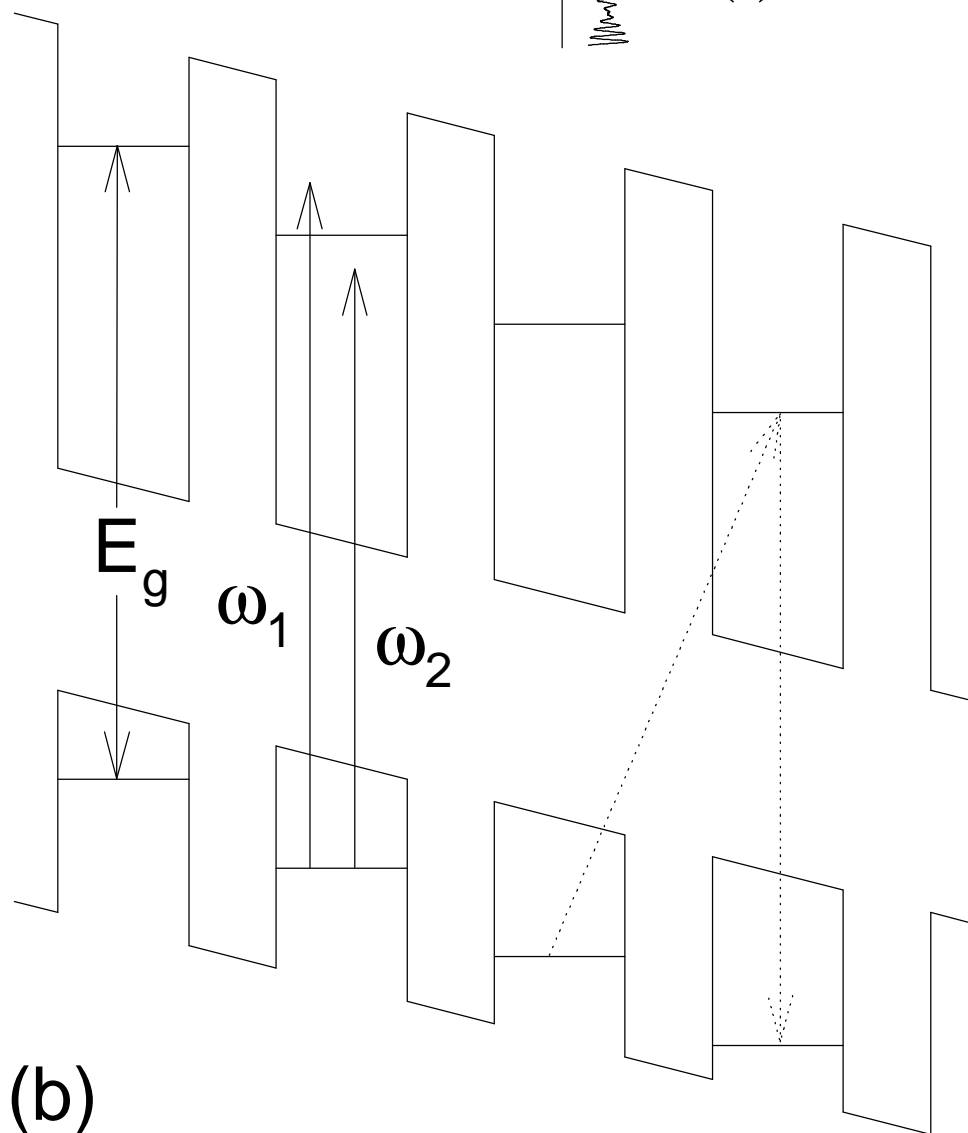
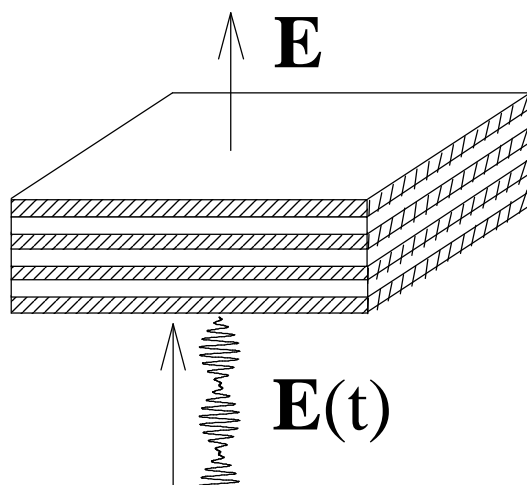
- [16] A. Mysyrowicz *et al.*, Phys. Rev. Lett. **56**, 2748 (1986); A. von Lehmen, D. S. Chemla, J. E. Zucker, and J. P. Heritage, Opt. Lett. **11**, 609 (1986); for a review, see, e.g., D. S. Chemla *et al.*, J. Lumin. **44**, 233 (1989).
- [17] M. M. Dignam and J. E. Sipe, Phys. Rev. Lett. **64**, 1797(1990).
- [18] C. P. Holfeld *et al.*, Phys. Rev. Lett. **81**, 874 (1998).
- [19] We have tried other initial conditions such as the Gaussian distribution and the Wannier-Stark state, the main effects are unchanged.
- [20] G. Bastard and R. Ferreira, in *Spectroscopy of Semiconductor Microstructures*, Vol. 206 of NATO *Advanced Study Institute*, Series B: Physics, edited by G. Fasol and A. Fasolino (Plenum Press, New York, 1989), P.333; M. M. Dignam, J. E. Sipe, and J. Shah, Phys. Rev. B **49**, 10 502 (1994).

FIG. 1. Schematics for (a) the DC- and bichromatic laser driven SSL system, and (b) the two components of the bichromatic laser (solid arrows), the WSL, and the virtual transitions leading to dynamical delocalization (dotted arrows).

FIG. 2. Quasienergies as functions of the optical coupling strength for 21 equally spaced k 's from 0 to $\pi/2$ with the following parameters: $\omega_{BO} = 2\omega = 10$ meV, and (a) $\Delta_c = 10\Delta_v = 30$ meV, (b) $\Delta_c = 10\Delta_v = 15$ meV. The perturbation results for $k = 0$ at the weak and strong optical coupling limits are plotted in dashed and dotted lines, respectively.

FIG. 3. Wave packet width (solid lines) as functions of time within the first ten periods for $2\chi/\omega = 0, 3.04,$ and 4.96 in (a), (b), and (c), respectively. Other parameters are the same as in Fig. 2 (b). In (b), the dashed line stands for wave packet width of a free Bloch electron which is initially localized, and the dotted line is the conduction electron population.

(a)



(b)

